HHS Public Access

Author manuscript

Nat Immunol. Author manuscript; available in PMC 2016 May 18.

Published in final edited form as:

Nat Immunol. 2016 January ; 17(1): 87–94. doi:10.1038/ni.3310.

Structural interplay between germline and adaptive recognition determines TCR-peptide-MHC cross-reactivity

Jarrett J. Adams[1,3,5], **Samanthi Narayanan**[2,5], **Michael E. Birnbaum**[1,5], **Sachdev S. Sidhu**[3], **Sydney J. Blevins**[4], **Marvin H. Gee**[1], **Leah V. Sibener**[1], **Brian M. Baker**[4], **David M. Kranz**[2], and **K. Christopher Garcia**[1,*]

[1]Howard Hughes Medical Institute, and Departments of Molecular and Cellular Physiology, and Structural Biology, Program in Immunology, Stanford University School of Medicine, Stanford, CA 94305

[2]Department of Biochemistry, University of Illinois at Urbana-Champaign, Urbana, IL 61801

[3]Banting and Best Department of Medical Research and Department of Molecular Genetics, University of Toronto, Donnelly CCBR, 160 College Street, Toronto, Ontario M5S 3E1, Canada

[4]Department of Chemistry & Biochemistry and the Harper Cancer Research Institute, University of Notre Dame, Notre Dame, IN 46556

Abstract

The T cell receptor - peptide-MHC interface is comprised of conserved and diverse regions, yet the relative contributions of each in shaping T cell recognition remain unclear. We isolated cross-reactive peptides with limited homology, allowing us to compare the structural properties of nine peptides for a single TCR-MHC pair. The TCR's cross-reactivity is rooted in highly similar recognition of an apical 'hotspot' position in the peptide, while tolerating significant sequence variation at ancillary positions. Furthermore, we find a striking structural convergence onto a germline-mediated interaction between TCR CDR1α and the MHC α2 helix of twelve TCR-pMHC complexes. Our studies suggest that TCR-MHC germline-mediated constraints, together with a focus on a small peptide hotspot, may place limits on peptide antigen cross-reactivity.

Antigen-specific T cell activation is initiated by αβ T cell receptor (TCR) engagement of short peptides presented by major histocompatability complex (MHC) proteins. In a structural symmetry that reflects the subdivided regions of the TCR and peptide-MHC

*Address correspondence to: K. Christopher Garcia, ; Email: kcgarcia@stanford.edu Tel# 650-498-7332

[5]These authors contributed equally to this work

Author Contributions

J.J.A., S.N., M.E.B., D.M.K., and K.C.G. conceived of the project. J.J.A., S.N., and M.E.B. performed experiments and analyzed data. All authors interpreted data, developed the concepts in the manuscript, and wrote and edited the manuscript.

Competing financial interests

The authors declare no competing financial interests.

Accession numbers

The coordinates and structure factors for the reported structures are deposited in the Protein Data Bank (PDB) under PDB IDs 4MS8, 4MVB, 4MXQ, 4N0C, and 4N5E.

(pMHC) surfaces, the TCR generally uses its germline derived CDR1 and 2 loops to contact the polymorphic but genetically encoded MHC helices, while the CDR3 loops, derived through V(D)J recombination, principally recognize the peptide bound in the MHC groove. Although exceptions exist[1–3], a large database of structures reveals a loosely consistent docking topology (+/− ~110°) whereby the TCR α chain sits over the N-terminal region of the peptide and α2 or β1 regions of Class I and Class II MHC respectively and the TCR β chain sits over the C-terminal region of the peptide and α1 regions of both MHC classes [2].

The forces that shape TCR-pMHC docking topology and cross-reactivity have been extensively studied, but without clear resolution[2]. With respect to docking topology, there has been significant debate about structural evidence for TCR bias towards MHC, and in particular, whether structurally similar interactions between germline-derived TCR CDR1 and 2 amino acids and conserved residues on MHC α helices are genetically encoded and evolutionarily conserved signatures of MHC restriction[1, 2, 4–10]. This debate has been influenced by the observation of structural variances, or adaptability, in TCR-pMHC interactions[2]. This adaptability can be local (e.g. restricted to individual loops and how they interface with MHC α helices) or global (e.g. resulting from alterations in TCR binding modes)[11–14].

The TCR-MHC interaction mode can be influenced by peptide or MHC changes, CDR3 loop alterations, or utilization of different Vα or Vβ domains[4, 5, 11, 15–23]. One difficulty in studying the determinants of TCR-pMHC docking topology is the complexity inherent in the TCR-pMHC interface, comprised of variable, composite surfaces that are functionally segregated but structurally and energetically cooperative[24]. Further complexity in the interpretation of structural data is added by the fact that thymic selection processes, including co-receptor involvement, may have pre-determined particular features of the interaction[25], shaping TCR-pMHC interactions observed in the context of peripheral T cells[26, 27]. In some contexts, TCRs can even recognize non-MHC antigens, a finding used to support the view that co-receptors alone can control the focus of TCRs on MHC ligands[28, 29]. These observations, however, do not rule out a role for a genetically imposed bias of TCRs towards MHC proteins, but imply that such biases do not impose absolute specificity.

TCR cross-reactivity has also been extensively studied, with highly divergent conclusions. On one hand, TCRs have the capacity to see many different peptide antigens presented by MHC[12, 30–32]. On the other hand, upon close inspection, TCRs may be less cross-reactive than previously appreciated as most cases of cross-reactivity appear to be explained by preservation of several key TCR contact residues in seemingly non-homologous peptides[23, 30, 33].

Previous work has considered TCR germline bias for MHC, cross-reactivity, and signaling independently. Taking into account structural and energetic interrelationships may prove beneficial for fully understanding TCR-pMHC recognition and signaling. Here, we use the murine 42F3 TCR, which recognizes the class I MHC H-2L^{d} [1], as a model system to further clarify the interplay between TCR cross-reactivity and germline specificity. We used peptide-MHC libraries displayed on yeast to screen recombinant, multimeric 42F3 TCR in a

cell-free environment, free of any constraints on binding, and isolated recognized peptides with limited homology to the cognate antigen.

By characterizing the binding, signaling and structural properties of peptide-TCR-MHC complexes with limited homology, we show that despite diversity in recognized peptide sequences, 42F3 TCR maintains highly similar 'hotspot' contacts with the most prominent up-facing peptide residues, resulting in a high degree of cross-reactivity while retaining specificity for key positions. Further, while the TCR adjusts its binding mode to engage different peptides, rather than seeing a spectrum of disparate binding solutions, the Vβ domain of the TCR ratchets between two "preferred" positions over the MHC α1 helix, while retaining an interaction between the MHC α2 helix and the TCR Vα that is nearly superimposable in 12 structures of a Vα3 TCR with H-2L^d. Based on these studies, we propose a model that functionally integrates TCR germline recognition and peptide cross-reactivity in which genetically-imprinted biases towards MHC help to "steer" TCR binding solutions but still permit the structural adaptability needed for cross-reactivity.

Results

A second generation yeast-displayed H-2L^d

We previously developed peptide libraries displayed by the murine class I MHC H-2L^d on yeast capable of identifying pMHC ligands for the alloreactive H-2L^d-specific TCR 42F3[1]. These libraries, based on the "mini-MHC" α1α2 scaffold termed H-2L^d-m31[34], utilized a single-chain configuration where the C-terminus of the mini-MHC was fused to the N-terminus of the 9 amino acid peptide[1]. Our selections identified mimeotopes to the cognate QL9 antigen (QLSPFPFDL), but all identified agonists shared obvious sequence homologies with QL9 that upon crystallographic study shared very similar TCR docking footprints[1]. We suspected the scaffold design might have limited our recovery of diverse peptide sequences, indicated by the very weak staining by 42F3 tetramers of H-2L^d-m31 fused to QL9.

Since we wished to find more divergent peptide sequences to better "stress test" TCR-pMHC recognition in the face of alternative peptide recognition chemistries, we developed a second-generation "mini-MHC" yeast display scaffold linking the C-terminus of the peptide to the MHC (Fig. 1a). The MHC included a Tyr84Ala mutation that opened a path at the C-terminal end of the groove to accommodate a linker, as was originally shown for pMHC single-chain trimers[35] (Supplementary Fig. 1a). However, in this orientation, the peptide C-terminus was far from the MHC N-terminus and would require a long connecting linker. Therefore, we circularly permuted (CP) the MHC to relocate the MHC N- and C-termini closer to the peptide C-terminus (Supplementary Fig. 1).

To circularly permute the MHC, we interrupted the sequence at a loop close to the peptide C-terminus, so that H-2L^d residue 120 became the new C-terminus, and Cys121 became the new N-terminus, while at the same time fusing the former C-terminal residue 180 to the former N-terminal residue 1 with a short GS linker (Supplementary Fig. 1). To avoid spontaneous intermolecular disulphide formation, the new N-terminus was substituted with mutation Cys121Ser. The peptide was then appended to the new N-terminus to complete the circular permutation. While yeast expressing QL9-m31r-CP stained positive for a cMyc

epitope tag, they were not recognized by either 2C- or 42F3-TCR tetramers, suggesting QL9-m31r-CP was displayed on the yeast surface but incorrectly folded (Supplementary Fig. 1b). To rescue the native fold, we evolved the m31r-CP design by creating a ~10^8 pool of variants produced by error prone PCR and selecting for gain-of-function mutations that recovered TCR recognition (Supplementary Fig. 1b). We found a subset of CP scaffold clones that contained only interface- and peptide-distal mutations and recognized both 2C- and 42F3-TCR tetamers. The clone with the brightest TCR-tetramer stains was m31r-CP-E3 (Supplementary Fig. 1c). The two selected mutations (Asp122Tyr and Ala136Thr) in this scaffold variant occurred in the proximity of the linker-MHC junction, perhaps accommodating the artificial linker or stabilizing the new MHC fold-initiating sequence (Supplementary Fig. 1c). We proceeded to construct new libraries to select for peptide presented by the circularly permuted MHC scaffold.

Peptide specificity of H-2L^d specific TCRs

We created a ‘random’ peptide library tethered to m31r-CP-E3 (Fig. 1a, Supplementary Fig. 1a–d). The diversity of this ‘random’ 9mer library was limited at the P2 (Pro) and the P9 (Phe, Ile, Leu, Met) anchor positions to reflect the natural preference for H-2L^d-presented peptides[36] (Fig. 1b). For selections, we used streptavidin (SA)-coated magnetic beads[30] saturated with biotinylated 42F3 TCR to enrich yeast clones from a library of 4.2x10^8 peptide variants (Fig. 1b–c, Supplementary Fig. 1e). We recovered a range of peptides unique in sequence from each other and the native QL9 agonist (Fig. 1c–d, Supplementary Fig. 1f). We sequenced several hundred clones from the final selected pool and observed a high degree of sequence diversity in all positions except P6 and P7. P7 was uniformly a large hydrophobic residue, as seen in QL9 (Fig. 1c–d). P6 exhibited a strong bias towards Pro and Gly, as seen in QL9, but allowed substitutions to Trp and Glu (Fig. 1c–d). The P5-P6-P7 sequence stretch in QL9 forms an arch that peaks at P7 and most intimately contacts CDR3β through apolar and van der Waals interactions[1]. Collectively, there appears to be selective pressure to preserve this interaction mode while allowing diverse chemistries at other positions (Fig. 1c–d). We sub-classified the sequences into related families and synthesized ten peptides for characterization, including five for structural characterization, whose sequences were suitably divergent from one another, from the cognate antigen QL9, and from the peptides derived from the previously published library[1].

Signaling properties of library-selected peptides

We screened both CD8$^-$ and CD8$^+$ 42F3 T cells for IL-2 production when stimulated with APCs presenting a subset of divergent peptides that arose from our second-generation selections, and compared them to the QL9 mimeotopes that arose from our first-generation libraries (Fig. 2a). Unlike the lone non-agonist peptide selected (p3A1-SPLDSLWWI) from the first-generation library, the majority of peptides selected from our second-generation library elicited substantial IL-2 responses in 42F3 transduced 58−/− cells at a 10μM dose on APCs (Fig. 2a). The synthetic peptide antigens presented a range of CD8 dependencies based on our initial screen as several second-generation peptides failed to stimulate or weakly stimulated in the absence of CD8 at this high peptide dose (Fig. 2a).

We titrated the IL-2 responses in $CD8^+$ 42F3 T cells for various agonist peptides with diverse sequences. Within this set, we observed IL-2 responses across a several log range of EC_{50} values (Fig. 2b, Supplementary Fig. 2, Table 1). Additionally, we assessed the affinity and kinetics of 42F3 TCR binding to each titrated peptide using surface plasmon resonance (Fig. 2b, Supplementary Fig. 3a–c, Table 1). As expected, we found that the highest affinity 42F3 TCR-pMHC complexes from our second-generation libraries were potent stimulators of IL-2 responses, but we also observed high-affinity ligands that produced partial IL-2 responses (pCPC5, pCPA12) as well as a moderate affinity ligand (p4B10) which potently stimulated IL-2 responses in $CD8^+$ 42F3 T cells (Fig. 2b).

The 42F3 agonists could be sub-divided into two categories. Potent agonists were classified as those peptides that elicited equally strong IL-2 responses in the presence and absence of CD8 co-receptor in our screen, and CD8-dependent agonists as those that required CD8 to maximally stimulate IL-2 production (Fig. 2a). While the potent agonists all produced high maximal IL-2 responses, the CD8-dependent agonists had a range of maximal responses including high (p5E8), medium (pCPA12) and low (QL9, pCPC5) on transduced $CD8^+$ 42F3 cells (Fig. 2b). One caveat to the stimulation data is that we do not know the relative loading efficiencies and binding affinities of the peptides to H-$2L^d$ on the cell surface, and these differences could play a role in the relative differences in stimulation potencies. However, all of the peptides have preserved optimal MHC binding anchors at P2 and P9, and are presented well in the single-chain format on yeast, so we suspect they are loaded on MHC. Collectively, the ability of the studied peptides to load in naturally-occurring H-$2L^d$, allow binding in affinity ranges expected for TCR-pMHC interactions, and induce signaling validates the use of the m31r-CP-E3 ‘mini’ H2-L^d as a system for discovering peptides of interest.

Peptide degeneracy of the 42F3 TCR

We crystallized five 42F3 TCR complexes bound to a mini-H-$2L^d$ scaffold (m31r) presenting the newly identified peptides (Fig. 3b, Supplementary Fig. 4a–b, Supplementary Table 1) and compared them to the ‘wild-type’ QL9 (Fig. 3a) and four previously characterized pMHC-42F3 complexes[1] (Fig. 3c, Supplementary Fig. 4c–d). The refolded m31r variant lacked the engineered linkers, circular permutation and synthetically evolved ‘stabilizing’ mutations, allowing us to study structures more representative of ‘naturally’ presented peptide, as when we tested for activity (Fig. 2). Importantly, every selected peptide assayed was recognized by 42F3 TCR in both presentation formats (i.e. covalently linked in the selection scaffold, and as free peptide refolded with MHC) (Figs. 2, 3). For each solved structure, the peptide backbone and side chain electron density were well defined (Supplementary Fig. 4).

To visualize the adaptive molecular determinants of peptide cross-reactivity by the 42F3 TCR CDR3s, we comprehensively compared the CDR3-peptide contacts of both the first- and second-generation complexes (Fig. 3b–c). Each peptide was recognized by a unique pattern of pair-wise contacts with the TCR CDR3 loops (Fig. 3b–c). Generally, the CDR3β loop contributed more to peptide recognition than the CDR3α, likely due to the arch in the peptide at residues lying underneath the CDR3β (Fig. 3b–c)[1]. In contrast, the CDR3α

contacts were in general fewer and more diverse in each complex, consistent with the lack of sequence specificity at the P1-P4 peptide positions (Fig. 1d, 3b–c). Overall, it appears that the arch in the C-terminal region of the peptide enforces close contact with 42F3 CDR3β, while the 'lower-lying' N-terminal peptide residues are more distant from CDR3α and permit more sequence diversity in this region. In two complexes (QL9, pCPB7), the CDR3α did not make contact with the peptide (Fig. 3b–c)[1]. Peptide conformation played a critical role in establishing contacts as the peptide backbone, rather than its side chains, were typically recognized by 42F3. For instance, 42F3 Lys95α frequently contacted the amide backbone of the presented peptide (5/9 complexes) while Asp95β frequently formed a hydrogen bond through its backbone carbonyl to the amide of the P8 position (4/9 complexes) (Fig. 3b–c).

The most consistent set of van der Waals contacts within this set of complexes arose from hydrophobic residues at the P7 peptide position to the Asp95-Ala96-Pro97 motif of the CDRβ3 loop (Fig. 3b–c). Since Pro97 restricts the dihedral angles of the loop, the CDR3β remains fixed in conformation in all nine complexes[1] (Fig. 3b–c). Other peptide positions whose sequences were biased in our enriched peptide pools (Fig. 1d) did not result in conserved contacts to the 42F3 TCR. For instance, the preferred acidic amino acid at P4 position correlated with potent IL-2 responses but failed to show conserved contacts across these complexes (Fig. 3b–c). In the pCPB9 and p4B10 complexes the acidic P4 side chain hydrogen bonded to Ser99α or Gly96α respectively (Fig. 3b–c). In the pCPB7 complex, the Glu4 position does not appear to make contact to the CDR3α loop (Fig. 3b–c). Similarly, while our structural set contained five complexes with peptides encoding a preferred P8-Asp, the contacts made by this residue vary from hydrogen bonding, to van der Waals contacts, to no contact to the TCR (Fig. 3b–c). Though we observed some amino acid preferences at the P4-P6 positions for 42F3 recognition (Fig. 1c–d), only the preferred hydrophobic P7 position resulted in conserved TCR-peptide interactions in agonist complexes (Fig. 3b–c).

Germline recognition in stimulatory receptor geometries

We next assessed how the TCR-MHC docking topology was modulated by the diverse agonist peptides derived from our selections. Combined, the nine 42F3 complexes (one non-agonist, eight agonist) produce three major docking topologies at angles of 84°, 64° and 27° (Fig. 4a). We previously characterized the 27° angle seen for a non-agonist peptide[1], so here we focus on the eight agonist peptides.

The most frequent docking mode, including each of the CD8-dependent agonists complexes (QL9, p5E8, pCPA12, pCPC5 and pCPE3) and partial agonist complexes (QL9, pCPA12, pCPC5 and pCPE3), was 64° relative to the peptide. Interestingly, two potent agonist pMHCs assumed an alternative docking geometry with a similar $V_{\alpha}3.3$ contact but a shifted $V_{\beta}8.3$ footprint, rotating the TCR to ~84° (Fig. 3B, 4A). These two peptides (pCPB7 and pCPB9; WPAEGGFQL and SPAEAGFFL) contained 6/9 identical residues, including a Glu at P4 and a Gly at P6. Residues at these positions differed from the peptides that exhibited the 64° docking angle (Fig. 3, 4a). One possibility is that the presence of a glycine at the P6 position provided sufficient flexibility of the peptide backbone to allow the TCR to pivot by

20°. Nevertheless, the slippage of the TCR-pMHC geometry from the 64° and 84° did not appear to affect the maximal stimulatory potential of the TCR-pMHC complexes, as agonists with 84° TCR docking geometries elicited IL-2 responses equivalent to that of the strongest 64° potent agonist p4B10 (Fig. 2, 4a). We therefore observed three peptide-induced docking modes by which the 42F3 TCR can engage H-2L^d, two of which were capable of maximally stimulating IL-2 responses and one (previously reported) that failed to stimulate 42F3 T cells[1].

Notably all agonist complexes, including previously published 2C TCR complexes with H-2L^d [12, 37], share a nearly atomically superimposable recognition motif mediated through the V$_\alpha$3.3 domain, in which Tyr31α and Tyr50α bury Tyr155 of the MHC and Ser51α hydrogen bonds to the Glu154 backbone (Fig. 4b, Supplementary Fig. 5a). The overall root-mean-square deviation (RMSD) of these three residues ranged from 0.9A to 2.2A when compared to the H-2L^d-QL9-42F3 pMHC-TCR complex. In contrast, the Vβ positions to cluster in two groups, either 64° or 84°. The 64° Vβ position consistently utilizes Asn30β, Tyr50β and Ala52β to engage the Gln72, Trp73, Ala76 and Arg97 of the α1 helix (Supplementary Fig. 5b). The 84° Vβ position utilizes Gln31β, Tyr50β and Gln71β of HV4 to contact Gln65, Lys68, Gln72, Val76 and Arg79 (Supplementary Fig. 5b). We therefore observe a pivot mechanism facilitating peptide cross-reactivity in which two Vβ contact motifs to the MHC accommodate diverse agonistic peptides while the dominant Vα3 germline contacts are conserved across all studied agonist complexes for 2C, 2C-variants and 42F3 TCRs recognizing H-2L^d (Fig. 4c, Supplementary Table 2).

Discussion

The data we present here, together with previously published structures of the 42F3 and 2C TCR and its variants bound to H-2L^d-QL9[1, 12, 37], constitute a structural database of twelve TCRs bearing a common germline element (V$_\alpha$3), engaging a common MHC allele (H-2L^d), but possessing differences in CDR3 sequences and recognizing distinct peptide sequences. Several conclusions about TCR cross-reactivity and germline recognition emerge from this analysis.

With respect to TCR cross-reactivity, we find that 42F3 can indeed recognize a wide range of peptides with limited homology to the cognate QL9. However, while this would appear to support the notion that the TCR is capable of ‘degenerate’ recognition of many diverse peptides in a biological milieu[31, 32, 38–41], a close inspection of the chemistry in the TCR-pMHC interfaces reveals a more nuanced reality. Despite sequence variability, 42F3 repeatedly focused on structurally and chemically similar elements of the peptides, most commonly using the CDR3β Asp-Ala-Pro motif to engage preferred hydrophobic residues at the P7 position. 42F3 recognition is therefore highly focused on a single apical peptide residue, with a wide range of chemistries and conformations used to accommodate the diversity at the remaining accessible positions. 42F3’s limited interaction with the peptide’s N-terminus relaxes overall peptide specificity, allowing for a larger number of peptide sequences to be recovered. It is possible, in fact likely, that an H-2L^d library that varied peptide lengths or MHC anchor residues could discover peptides that are seen with substantially different TCR binding solutions. However, we believe that our results reflect

the general properties of most TCR-pMHC interactions. The scope and nature of cross-reactivity is consistent with recent data that focused on TCRs recognizing class II MHC molecules[30]. Collectively these data suggest that TCRs are more specific than appreciated, and lead to a more granular definition of cross-reactivity as being rooted in highly specific peptide hotspots enabling relaxed specificities at ancillary positions.

The conclusions of these studies reflect a fundamental feature of protein-protein interfaces: engagement of a small number of structurally and energetically important “hotspots,” typically near the interface center, surrounded by weaker and more diverse peripheral interactions[17, 30, 42]. Inspection of the amino acid sequences of peptides recognized by 42F3 in the absence of structural information suggests degeneracy, while in fact recognition is focused on key features shared among recognized peptides. Although CDR3-peptide hotspots have been previously discussed in TCR-pMHC interfaces[17, 43], the observation that the same hotspot is repeatedly engaged in the 42F3 system, together with visualization of how sequence diversity is tolerated, allows a better understanding of the nature of TCR cross-reactivity. This mechanism ensures the capacity to engage large numbers of diverse peptides, while retaining specificity for at least one structural and chemically homologous position. We suggest the parsing of the TCR-pMHC interface into hotspot and non-hotspot residues contributes significantly to the “dichotomy” of cross-reactivity and specificity that characterizes TCR recognition[2, 30].

With respect to germline recognition, we observe a striking, near atomic superimposition of the interaction between V_α3.3 and the H-2L^d α2 helix in 12 structures with different peptides, Vβ segments, and CDR3 loops. The repeated observation of this interaction, in the presence of considerable local and global structural variation, likely reflects the imprint of TCR-MHC co-evolution, in this case a favorable “patch” between V_α3.3 and H-2L^d. In the case of 42F3, these interactions appear to dominate over the Vβ interactions, permitting the observed “ratcheting” of Vβ along the α1 helix (dominant roles for α chains in TCR binding have been observed previously) [44]. The inherent adaptability or “give” available to TCR-MHC germline interactions is illustrated by the p3A1 non-agonist peptide, whose Trp-Trp motif occludes the preferred V_α3.3 docking site, resulting in a ‘peptide-centric geometry’[1]. Similar circumstances might be found with long or otherwise unusually ‘bulged’ peptides[22, 45].

Our observations suggest an interplay between TCR-MHC germline bias and its potential influence on cross-reactivity. It has been shown that alterations in TCR docking modes can facilitate cross-reactivity[1, 11–13, 33], and that CDR3 loops can affect TCR-MHC contacts through ‘CDR3 editing’[46]. Consistent with earlier results, we also observe that different peptides can yield different binding modes even with the same TCR and MHC. Yet rather than seeing a spectrum of binding topologies that would be expected from a purely opportunistic system (e.g., antibody-antigen interactions), we observe distinct, discrete binding modes for peptides in the form of “ratcheting” of the 42F3 Vβ along the H-2L^d α1 helix or equivalently, preferences of 42F3 for particular binding orientations. The existence of these structural preferences, even in the case of the alloreactive TCR-MHC pair of 42F3 and H-2L^d that did not encounter each other during T cell development, strongly support co-evolution between TCR and MHC. Importantly though, these observations also support the

presence of a genetically encoded adaptability that can facilitate cross-reactivity. In this case, the orientations of the 42F3 Vβ domain likely stem from a combination of germline-encoded attractive and repulsive interactions at preferred and non-preferred orientations, respectively. From these data, we propose a model for TCR engagement that integrates germline bias and peptide recognition. TCRs are clearly adaptable, even capable of engaging in non-productive binding modes, and under certain circumstances, of binding non-MHC ligands[1, 28, 29, 47]. We suggest the existence of preferred but weak Vα or Vβ interaction points along MHC helices that bias TCRs towards, but do not obligate, discrete binding solutions. Chemically, this could arise from the incorporation of multi-functional amino acids such as tyrosine and the strategic placement of charges or hydrogen bond donors and acceptors as seen with the interaction points between 42F3 and H-2L^d. The resulting structural biases would help to "focus" binding while still permitting structural adaptations as the CDR3 loops accommodate peptide hotspots. In this way, the mechanisms of TCR cross-reactivity and germline bias are cooperative processes in shaping recognition of peptide-MHC complexes.

On-line Methods

Design and selection of H-2L^d m31r-CP

In order to recover larger arrays of peptide from yeast selections, we optimized several features of our original yeast display scaffold[1]. Of the five mutations, three (Asn30Asp, Ala49Asp and Lys131Arg) arose distal from the TCR and peptide binding surfaces; however, two mutations arose in the bottom of the peptide-binding groove (Trp97Arg) or on the surface of the α1 helix (Ile66Val).

To produce a closer H-2L^d mimic for display, we reverted the peptide proximal mutations back to WT (Ile66 and Trp97) to produce an m31r variant that contained three peptide-distal, TCR-distal mutations and synthesized the mini-MHC m31r-CP encoding a tethered QL9 peptide (Genscript). The QL9-m31r-CP construct linked the C terminus of the QL9 peptide to the N-terminus of the H-2L^d α2 domain (amino acids 121–180) via a 12 amino acid gly-ser (GGGGS) linker, and then the C terminus of the H-2L^d α2 domain to the N-terminus of the H-2L^d α1 domain (amino acids 1–120) via a 6 amino acid Gly-Ser linker. The construct was cloned into the pYAL vector using NheI and HindIII restriction sites. Yeast expressing this construct stained with an anti-Myc epitope antibody (Cell Signaling, clone 9B11), but did not stain with 42F3 or 2C TCR tetramers.

To create a functional version of m31r-CP, Variants of QL9-tethered scaffolds were amplified from 50ng m31r-CP template DNA using the GeneMorph II Random Mutagenesis kit and co-transformed into EBY100 in a 1:5μg vector:insert ratio as previously described[1, 30]. Yeast titers indicated that the error-prone library contained >10^8 transformants. Selections were carried out using magnetic bead selection strategy.

The selections for a functional variant of m31r-CP were conducted with both 2C and 42F3 TCRs to ensure the library did not converge to a TCR-specific MHC construct. Briefly, induced yeast libraries were negatively selected with 500ul αPE-magnetic beads (Miltenyi) using a LS column (Miltenyi) before tetramer-positive selections. Positive selections were carried out using preformed 2C-tetramers at 500nM tetramer concentration in PBS + 0.5%

BSA (PBS-BSA) and gently mixed at 4°C for 2.5hrs. Cells were washed three times with PBS-BSA and mixed with 500μlαPE-magnetic beads (Miltenyi) in 5ml PBS-BSA. Beads were gently mixed at 4°C for 20min, washed twice to remove unbound beads and added to a LS-column magnetic column (Miltenyi). After washing with 3 column volumes of PBS-BSA, the column was then removed from the magnetic field and bound cells eluted in 5ml of PBS-BSA. From the eluted yeast, 50μl of cells were put aside for flow analysis and cell count on a C6 Flow cytometer (Accuri). The cells were then recovered in SDCAA overnight at 30°C, before diluting into 5ml SGCAA induction media. Cells were cultured at 20°C for 48hrs before the selection process was repeated. For all subsequent rounds of selections, 10 times the eluted cells from the previous round were negatively selected using αPE-magnetic beads and positively selected using 500nM 2C- or 42F3-tetramer and 50μl of αPE magnetic beads in 1ml volumes. Populations were enriched until the 100nM TCR-tetramer stained >10% of the yeast population for both TCR specificities. Individual clones were picked, analyzed for binding by flow cytometry using 100nM TCR-tetramer. Clonal DNA vectors were extracted from yeast using Zymoprep Yeast Plasmid Miniprep II kit (Zymogen) and amplified in DH5α *E. coli* for sequencing (Sequetech).

Yeast displayed pMHC library and selections

The yeast display scaffold m31r-CP-E3 was converted into a library template by introducing a stop codon into the QL9 sequence. Synthetic primers encoding 5' NNK CCC NNK NNK NNK NNK NNK NNK HTK 3' library were used to amplify peptide variants tethered to m31r-CP-E3 from the stop template and purified by gel extraction (Qiagen). Amplicons were used as a template for a second PCR amplification step, in which an additional 50bp complimentary to 5' of the NheI and 3' to the HindIII sites in the pYAL vector were added to the peptide variants. μg of purified amplicon (Qiagen) was mixed together with digested pYAL (NheI/HindIII) in a 2.5:1 mass ratio and electroporated in EBY100 yeast. Titers of the initial yeast libraries indicated a total of $4.2x10^8$ clones in the library. Biotinylated 42F3 TCR was expressed and purified as previously described[1]. TCRs were mixed with 250μl of SA-magnetic beads (Miltneyi) at a concentration of 400nM TCR and incubated a 4°C for 20min to form pre-coated TCR-magnetic beads. Before positive selection, yeast populations underwent negative selection on an LS column in the presence of uncoated SA-magnetic beads (Miltenyi). TCR-magnetic beads were then added to the precleared yeast population before positive tetramer selection on an LS column (Miltenyi). Subsequent selections on enriched pools were carried out on LS columns (Miltenyi) using 50μl of precoated TCR-magnetic beads. Enrichments were analyzed using 100nM TCR-tetramer throughout rounds of enrichment. Upon enrichment of >10% TCR-tetramer staining within the co-selected yeast population, a final 'polishing' round of enrichment was carried out using multimeric 42F3 TCR. Individual clones were analyzed for 100nM TCR-tetramer binding by flow cytometry and sequenced as previously described[1].

Protein expression, purification, and crystallization

For selections, biotinylated 2C and 42F3 TCRs were produced and biotinylated by coexpression of TCRα and TCRβ viruses in High Five *Trichopulsia ni* insect cells. The α and β chains were co-secreted with BirA ligase into media in the presence of 100μM biotin supplemented to the media Insect-XPRESS (Lonza) as previously described[1].

42F3 was purified and refolded from *E. coli* inclusion bodies as previously described[1]. An *E. coli*-expressed m31r refold construct was created by mutating R97W and V66I in the H-2L^d 'mini-MHC' protein previously described[1]. Peptides were synthesized (GenScript) and refolded at 20μM concentration in the presence of 300mg m31r as previously described[1]. After dialysis, pMHC were precipitated using 60% saturation of ammonium sulfate a 4°C and purified by size exclusion on a Superdex 200 in HEPES-buffered saline. The A_{280} was used to determine the concentration of TCR and pMHC and proteins were concentrated in a 1:1 molar ratio to 150μM for crystal screens.

All crystals were formed in sitting drops using a vapor diffusion method. The 42F3-pCPA12-m31r complex was crystallized in 16% PEG 3350, 100mM TRIS, pH 7.5 and 200mM magnesium nitrate and cryogenically frozen in liquid nitrogen in crystallization buffer with 20% ethylene glycol. The 42F3-pCPB7-m31r complex was crystallized in 25% PEG 3350, 100mM BIS-TRIS pH 5.5 and 200mM ammonium acetate and cryogenically frozen in liquid nitrogen in crystallization buffer with 10% ethylene glycol. The 42F3-pCPB9-m31r complex was crystallized in 20% PEG 4000, 100mM TRIS pH 8.0 200mM sodium chloride and cryogenically frozen in liquid nitrogen in crystallization buffer with 15% ethylene glycol. The 42F3-pCPC5-m31r complex was crystallized in 14% PEG 3350, 100mM BIS-TRIS, pH 7.0 and 200mM magnesium nitrate and cryogenically frozen in liquid nitrogen in crystallization buffer with 20% ethylene glycol. The 42F3-pCPE3-m31r complex was crystallized in 17% PEG 3350 and 100mM BIS-TRIS, pH 6.6 and 200mM magnesium nitrate and cryogenically frozen in liquid nitrogen in crystallization buffer with 20% ethylene glycol.

All crystallographic data were collected at the Stanford Synchrotron Radiation Lightsource (Stanford, CA, USA) beamline 12-2. Datasets were indexed and scaled in MOSFLM/SCALA[48] with the exception of pCPB7 construct, which was indexed and scaled in HKL2000[49]. All datasets were phased by molecular replacement with PHASER[50] by searching for TCR and pMHC independently (PDB accession 3TFK), refined using PHENIX[51] and modified using COOT[52]. Structural analysis, alignments and image rendering were carried out in PYMOL[53].

T cell stimulations

All peptides were diluted to 50mM in DMSO. Transduced LM1.8-L^{d}W97R cells were grown in RPMI with 10% FBS with penicillin, streptomycin and L-glutamine to a confluency of 90% in T75 flasks. T cell stimulations were carried out as previously described[1]. Briefly, LM1.8-L^{d}W97R ($5x10^4$ cells) and peptides diluted in RPMI were incubated in a 1:1 effector-to-target ratio with CD8αβ$^-$ or CD8αβ$^+$ 58−/− lines transduced to express 2C-m33 or 42F3 TCRs for 20 h at 37°C. Supernatants were analyzed for IL-2 release using a HRP-colormetric ELISA (BD Pharmingen).

The 42F3-transduced cell lines were generated as previously described[1] using T cell hybridoma cell line 58−/− (TCRα−, TCRβ−) with and without CD8αβ. The 58−/− cell line was provided to the lab of D.M. Kranz by Sean O'Herrin. These cell lines have not been tested for mycoplasma contamination, however no contamination was observed during generation of these cell lines or in their subsequent culturing and maintenance.

The antigen presenting cell line used in this study, LM1.8-L^{d}W97R, is an L cell fibroblast cell line that was provided for use by Janet M. Connolly. This cell line was not tested for mycoplasma contamination during its use in the lab of D.M. Kranz, however no contamination was observed during the culturing or maintenance of this cell line.

The antibodies used in T cell activation studies include anti-mouse CD3e (Clone 145-2C11 from BD Pharmingen), purified rat-anti-mouse IL-2 (Clone JES6-1A12 from BD Pharmingen), and biotinylated rat-anti-mouse IL-2 (Clone JES6-5H4 from BD Pharmingen). Anti-mouse TCR constant-region Beta antibody (Clone H57-597 from BD Pharmingen) was used to detect the expression of the 42F3 TCR on the surface of transduced 58−/− during generation of the cell line created via retroviral transduction.

Supplementary Material

Refer to Web version on PubMed Central for supplementary material.

Acknowledgments

We thank N. Goriatcheva, E. Ozkan, D.Wittrup, E. Newell, N. Jarvik, and M.McLaughlin for helpful discussions. JJA was supported by a Canadian Institutes of Health Research (CIHR) post-doctoral fellowship, MEB was supported by National Science Foundation and Stanford Graduate pre-doctoral fellowships. This work was supported by NIH grants AI48540 (KCG) and GM55767 (DMK). KCG is an Investigator of the Howard Hughes Medical Institute. Use of the Stanford Synchrotron Radiation Lightsource, SLAC National Accelerator Laboratory, is supported by the U.S. Department of Energy, Office of Science, Office of Basic Energy Sciences under Contract No. DE-AC02-76SF00515. The SSRL Structural Molecular Biology Program is supported by the DOE Office of Biological and Environmental Research, and by the National Institutes of Health, National Institute of General Medical Sciences (including P41GM103393).

References

1. Adams JJ, Narayanan S, Liu B, Birnbaum ME, Kruse AC, Bowerman NA, et al. T Cell Receptor Signaling Is Limited by Docking Geometry to Peptide-Major Histocompatibility Complex. Immunity. 2011; 35(5):681–693. [PubMed: 22101157]
2. Rossjohn J, Gras S, Miles JJ, Turner SJ, Godfrey DI, McCluskey J. T cell antigen receptor recognition of antigen-presenting molecules. Annu Rev Immunol. 2015; 33:169–200. [PubMed: 25493333]
3. Beringer DX, Klejwegt FS, Wiede F, van der Slik AR, Loh KL, Petersen J, et al. T cell receptor reversed polarity recognition of a self-antigen major histocompatibility complex. Nat Immunol. 2015; 16(11)
4. Dai S, Huseby ES, Rubtsova K, Scott-Browne J, Crawford F, Macdonald WA, et al. Crossreactive T Cells spotlight the germline rules for alphabeta T cell-receptor interactions with MHC molecules. Immunity. 2008; 28(3):324–334. [PubMed: 18308592]
5. Feng D, Bond CJ, Ely LK, Maynard J, Garcia KC. Structural evidence for a germline-encoded T cell receptor-major histocompatibility complex interaction 'codon'. Nat Immunol. 2007; 8(9):975–983. [PubMed: 17694060]
6. Garcia KC, Adams JJ, Feng D, Ely LK. The molecular basis of TCR germline bias for MHC is surprisingly simple. Nat Immunol. 2009; 10(2):143–147. [PubMed: 19148199]
7. Marrack P, Scott-Browne JP, Dai S, Gapin L, Kappler JW. Evolutionarily conserved amino acids that control TCR-MHC interaction. Annu Rev Immunol. 2008; 26:171–203. [PubMed: 18304006]
8. Rangarajan S, Mariuzza RA. T cell receptor bias for MHC: co-evolution or co-receptors? Cellular and molecular life sciences : CMLS. 2014; 71(16):3059–3068. [PubMed: 24633202]

9. Scott-Browne JP, White J, Kappler JW, Gapin L, Marrack P. Germline-encoded amino acids in the alphabeta T-cell receptor control thymic selection. Nature. 2009; 458(7241):1043–1046. [PubMed: 19262510]
10. Van Laethem F, Tikhonova AN, Singer A. MHC restriction is imposed on a diverse T cell receptor repertoire by CD4 and CD8 co-receptors during thymic selection. Trends Immunol. 2012; 33(9): 437–441. [PubMed: 22771139]
11. Borbulevych OY, Santhanagopolan SM, Hossain M, Baker BM. TCRs used in cancer gene therapy cross-react with MART-1/Melan-A tumor antigens via distinct mechanisms. J Immunol. 2011; 187(5):2453–2463. [PubMed: 21795600]
12. Colf LA, Bankovich AJ, Hanick NA, Bowerman NA, Jones LL, Kranz DM, et al. How a single T cell receptor recognizes both self and foreign MHC. Cell. 2007; 129(1):135–146. [PubMed: 17418792]
13. Yin L, Huseby E, Scott-Browne J, Rubtsova K, Pinilla C, Crawford F, et al. A single T cell receptor bound to major histocompatibility complex class I and class II glycoproteins reveals switchable TCR conformers. Immunity. 2011; 35 (1):23–33. [PubMed: 21683626]
14. Stadinski BD, Trenh P, Smith RL, Bautista B, Huseby PG, Li G, et al. A role for differential variable gene pairing in creating T cell receptors specific for unique major histocompatibility ligands. Immunity. 2011; 35(5):694–704. [PubMed: 22101158]
15. Borbulevych OY, Piepenbrink KH, Gloor BE, Scott DR, Sommese RF, Cole DK, et al. T cell receptor cross-reactivity directed by antigen-dependent tuning of peptide-MHC molecular flexibility. Immunity. 2009; 31(6):885–896. [PubMed: 20064447]
16. Burrows SR, Chen Z, Archbold JK, Tynan FE, Beddoe T, Kjer-Nielsen L, et al. Hard wiring of T cell receptor specificity for the major histocompatibility complex is underpinned by TCR adaptability. Proc Natl Acad Sci U S A. 2010; 107(23):10608–10613. [PubMed: 20483993]
17. Degano M, Garcia KC, Apostolopoulos V, Rudolph MG, Teyton L, Wilson IA. A functional hot spot for antigen recognition in a superagonist TCR/MHC complex. Immunity. 2000; 12(3):251–261. [PubMed: 10755612]
18. Ding YH, Baker BM, Garboczi DN, Biddison WE, Wiley DC. Four A6-TCR/peptide/HLA-A2 structures that generate very different T cell signals are nearly identical. Immunity. 1999; 11(1): 45–56. [PubMed: 10435578]
19. Garcia KC, Degano M, Pease LR, Huang M, Peterson PA, Teyton L, et al. Structural basis of plasticity in T cell receptor recognition of a self peptide-MHC antigen. Science. 1998; 279(5354): 1166–1172. [PubMed: 9469799]
20. Garcia KC, Degano M, Stanfield RL, Brunmark A, Jackson MR, Peterson PA, et al. An ab T cell receptor structure at 2. 5A and its orientation in the TCR-MHC complex. Science. 1996; 274(5285):209–219. [PubMed: 8824178]
21. Huseby ES, White J, Crawford F, Vass T, Becker D, Pinilla C, et al. How the T cell repertoire becomes peptide and MHC specific. Cell. 2005; 122(2):247–260. [PubMed: 16051149]
22. Liu YC, Miles JJ, Neller MA, Gostick E, Price DA, Purcell AW, et al. Highly divergent T-cell receptor binding modes underlie specific recognition of a bulged viral peptide bound to a human leukocyte antigen class I molecule. J Biol Chem. 2013; 288(22):15442–15454. [PubMed: 23569211]
23. Mazza C, Auphan-Anezin N, Gregoire C, Guimezanes A, Kellenberger C, Roussel A, et al. How much can a T-cell antigen receptor adapt to structurally distinct antigenic peptides? EMBO Journal. 2007; 26(7):1972–1983. [PubMed: 17363906]
24. Piepenbrink KH, Blevins SJ, Scott DR, Baker BM. The basis for limited specificity and MHC restriction in a T cell receptor interface. Nat Commun. 2013; 4:1948. [PubMed: 23736024]
25. Yin Y, Wang XX, Mariuzza RA. Crystal structure of a complete ternary complex of T-cell receptor, peptide-MHC, and CD4. Proc Natl Acad Sci U S A. 2012; 109(14):5405–5410. [PubMed: 22431638]
26. Correia-Neves M, Waltzinger C, Mathis D, Benoist C. The shaping of the T cell repertoire. Immunity. 2001; 14(1):21–32. [PubMed: 11163227]
27. Starr TK, Jameson SC, Hogquist KA. Positive and negative selection of T cells. Annu Rev Immunol. 2003; 21:139–176. [PubMed: 12414722]

28. Alajez NM, Schmielau J, Alter MD, Cascio M, Finn OJ. Therapeutic potential of a tumor-specific, MHC-unrestricted T-cell receptor expressed on effector cells of the innate and the adaptive immune system through bone marrow transduction and immune reconstitution. Blood. 2005; 105(12):4583–4589. [PubMed: 15746083]
29. Van Laethem F, Sarafova SD, Park JH, Tai X, Pobezinsky L, Guinter TI, et al. Deletion of CD4 and CD8 coreceptors permits generation of alphabetaT cells that recognize antigens independently of the MHC. Immunity. 2007; 27(5):735–750. [PubMed: 18023370]
30. Birnbaum ME, Mendoza JL, Sethi DK, Dong S, Glanville J, Dobbins J, et al. Deconstructing the peptide-MHC specificity of T cell recognition. Cell. 2014; 157(5):1073–1087. [PubMed: 24855945]
31. Sewell AK. Why must T cells be cross-reactive? Nat Rev Immunol. 2012; 12(9):669–677. [PubMed: 22918468]
32. Wooldridge L, Ekeruche-Makinde J, van den Berg HA, Skowera A, Miles JJ, Tan MP, et al. A single autoimmune T cell receptor recognizes more than a million different peptides. J Biol Chem. 2012; 287(2):1168–1177. [PubMed: 22102287]
33. Felix NJ, Donermeyer DL, Horvath S, Walters JJ, Gross ML, Suri A, et al. Alloreactive T cells respond specifically to multiple distinct peptide-MHC complexes. Nat Immunol. 2007; 8(4):388–397. [PubMed: 17322886]
34. Jones LL, Brophy SE, Bankovich AJ, Colf LA, Hanick NA, Garcia KC, et al. Engineering and characterization of a stabilized alpha1/alpha2 module of the class I major histocompatibility complex product Ld. J Biol Chem. 2006; 281(35):25734–25744. [PubMed: 16815841]
35. Mitaksov V, Truscott SM, Lybarger L, Connolly JM, Hansen TH, Fremont DH. Structural engineering of pMHC reagents for T cell vaccines and diagnostics. Chemistry & biology. 2007; 14(8):909–922. [PubMed: 17719490]
36. Udaka K, Wiesmuller KH, Kienle S, Jung G, Tamamura H, Yamagishi H, et al. An automated prediction of MHC class I-binding peptides based on positional scanning with peptide libraries. Immunogenetics. 2000; 51(10):816–828. [PubMed: 10970096]
37. Jones LL, Colf LA, Stone JD, Garcia KC, Kranz DM. Distinct CDR3 conformations in TCRs determine the level of cross-reactivity for diverse antigens, but not the docking orientation. J Immunol. 2008; 181(9):6255–6264. [PubMed: 18941216]
38. Mason D. A very high level of crossreactivity is an essential feature of the T-cell receptor. Immunol Today. 1998; 19(9):395–404. [PubMed: 9745202]
39. Maynard J, Petersson K, Wilson DH, Adams EJ, Blondelle SE, Boulanger MJ, et al. Structure of an autoimmune T cell receptor complexed with class II peptide-MHC: insights into MHC bias and antigen specificity. Immunity. 2005; 22 (1):81–92. [PubMed: 15664161]
40. Pinilla C, Martin R, Gran B, Appel JR, Boggiano C, Wilson DB, et al. Exploring immunological specificity using synthetic peptide combinatorial libraries. Curr Opin Immunol. 1999; 11(2):193–202. [PubMed: 10322159]
41. Wilson DB, Wilson DH, Schroder K, Pinilla C, Blondelle S, Houghten RA, et al. Specificity and degeneracy of T cells. Mol Immunol. 2004; 40(14–15):1047–1055. [PubMed: 15036909]
42. Bogan AA, Thorn KS. Anatomy of hot spots in protein interfaces. Journal of molecular biology. 1998; 280(1):1–9. [PubMed: 9653027]
43. Gagnon SJ, Borbulevych OY, Davis-Harrison RL, Baxter TK, Clemens JR, Armstrong KM, et al. Unraveling a hotspot for TCR recognition on HLA-A2: evidence against the existence of peptide-independent TCR binding determinants. J Mol Biol. 2005; 353(3):556–573. [PubMed: 16197958]
44. Yokosuka T, Takase K, Suzuki M, Nakagawa Y, Taki S, Takahashi H, et al. Predominant role of T cell receptor (TCR)-alpha chain in forming preimmune TCR repertoire revealed by clonal TCR reconstitution system. J Exp Med. 2002; 195(8):991–1001. [PubMed: 11956290]
45. Tynan FE, Burrows SR, Buckle AM, Clements CS, Borg NA, Miles JJ, et al. T cell receptor recognition of a 'super-bulged' major histocompatibility complex class I-bound peptide. Nature Immunology. 2005; 6(11):1114–1122. [PubMed: 16186824]
46. Deng L, Langley RJ, Wang Q, Topalian SL, Mariuzza RA. Structural insights into the editing of germ-line-encoded interactions between T-cell receptor and MHC class II by Valpha CDR3. Proc Natl Acad Sci U S A. 2012; 109(37):14960–14965. [PubMed: 22930819]

47. Tikhonova AN, Van Laethem F, Hanada KI, Lu J, Pobezinsky LA, Hong C, et al. alphabeta T Cell Receptors that Do Not Undergo Major Histocompatibility Complex-Specific Thymic Selection Possess Antibody-like Recognition Specificities. Immunity. 2012; 36(1):79–91. [PubMed: 22209676]

48. Leslie AGW. Recent changes to the MOSFLM package for processing film and image plate data. Joint CCP4 + ESF-EAMCB Newsletter on Protein Crystallography. 1992; 26

49. Otwinowski, Z.; Minor, W.; Carter, Charles W, Jr. Methods in Enzymology. Vol. 276. Academic Press; 1997. [20] Processing of X-ray diffraction data collected in oscillation mode; p. 307-326.

50. McCoy AJ. Solving structures of protein complexes by molecular replacement with Phaser. Acta Crystallogr D Biol Crystallogr. 2007; 63(Pt 1):32–41. [PubMed: 17164524]

51. Adams PD, Afonine PV, Bunkoczi G, Chen VB, Davis IW, Echols N, et al. PHENIX: a comprehensive Python-based system for macromolecular structure solution. Acta Crystallogr D Biol Crystallogr. 2010; 66(Pt 2):213–221. [PubMed: 20124702]

52. Emsley P, Cowtan K. Coot: model-building tools for molecular graphics. Acta Crystallographica Section D-Biological Crystallography. 2004; 60(Pt 12 Pt 1):2126–2132.

53. DeLano, WL. The PyMol Molecular Graphics System. 2002.

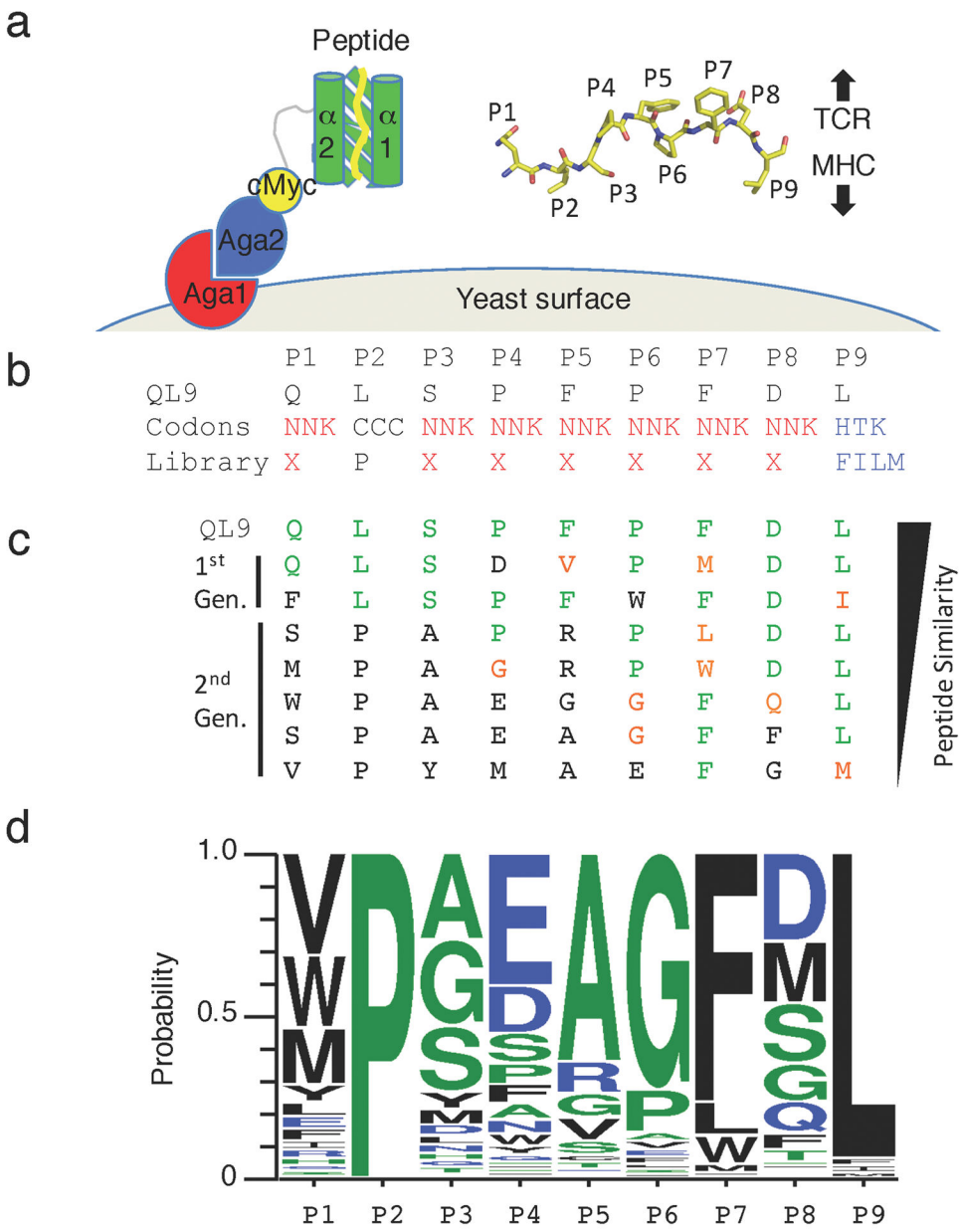

Fig. 1.

TCR selections of a circularly-permuted H-2L^d- yeast displayed library

(**a**) Cartoon schematic of the circularly permuted mini-MHC m31r-CP and its presentation on the surface of EBY100 yeast as an Aga2 fusion protein. Inset is a stick schematic of the tethered QL9 peptide. Peptide positions are labeled accordingly and the general orientation of the TCR and MHC relative to the peptide is indicated with arrows. (**b**) The amino acid composition design of a 'random' peptide library where the P2 and P9 anchor positions are weighted to specific amino acids and the sequence of a natively displayed peptide QL9. (**c**) Representative peptides recovered by selection of first- and second-generation H-2L^d peptide libraries with 42F3 TCR multimers. Amino acids at a given position identical to those in QL9 are colored green. Amino acids with similar properties to QL9 are colored

orange. Non-homologous resides are colored black. (**d**) The positional amino acid probabilities of peptides recovered from the enriched yeast populations specific for 42F3 TCR. Redundant peptide clones are represented once.

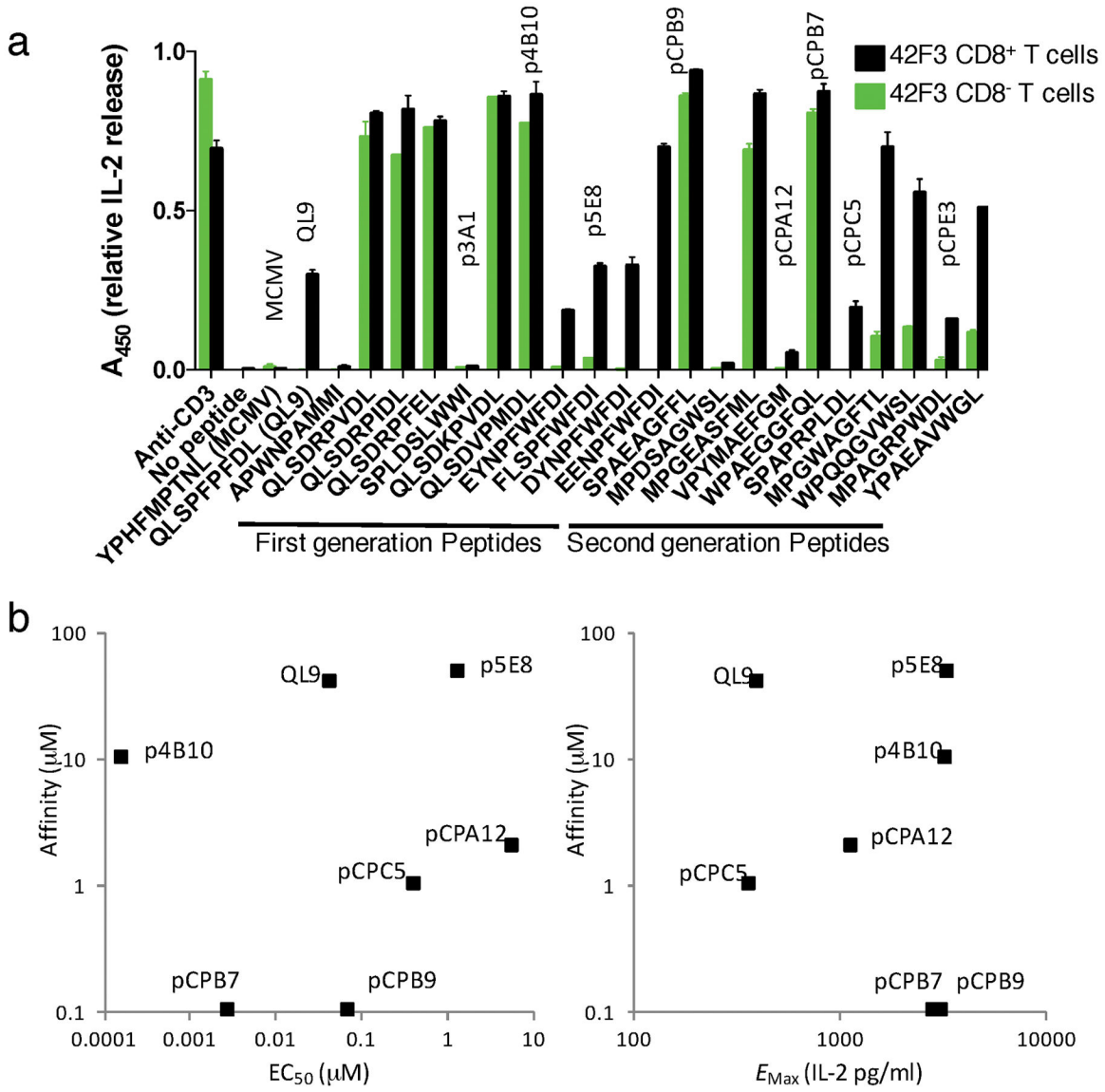

Fig. 2.

Signaling properties of synthetic peptide antigens

(**a**) IL-2 response screen of the $CD8^+$ (black bars) and $CD8^-$ (green bars) 42F3 T cells to APCs in the presence of 10μM synthesized peptide from first-generation (left) and second-generation (right) yeast displayed pMHC libraries. Data is represented as mean ± s.e.m. relative A450, normalized to anti-CD3 stimulation condition n=2 of technical replicates. (**b**) Scatterplots showing a wide range in affinities and activities, but little correlation between the IL-2 EC50 (left) or maximal IL-2 response (Emax) (right, as shown in Supplementary Fig. 2) of $CD8^+$ 42F3 T with affinity of the 42F3-pMHC interactions. pCPE3 is a weak agonist for which EC50 and Emax were not determined, and was therefore omitted from this analysis.

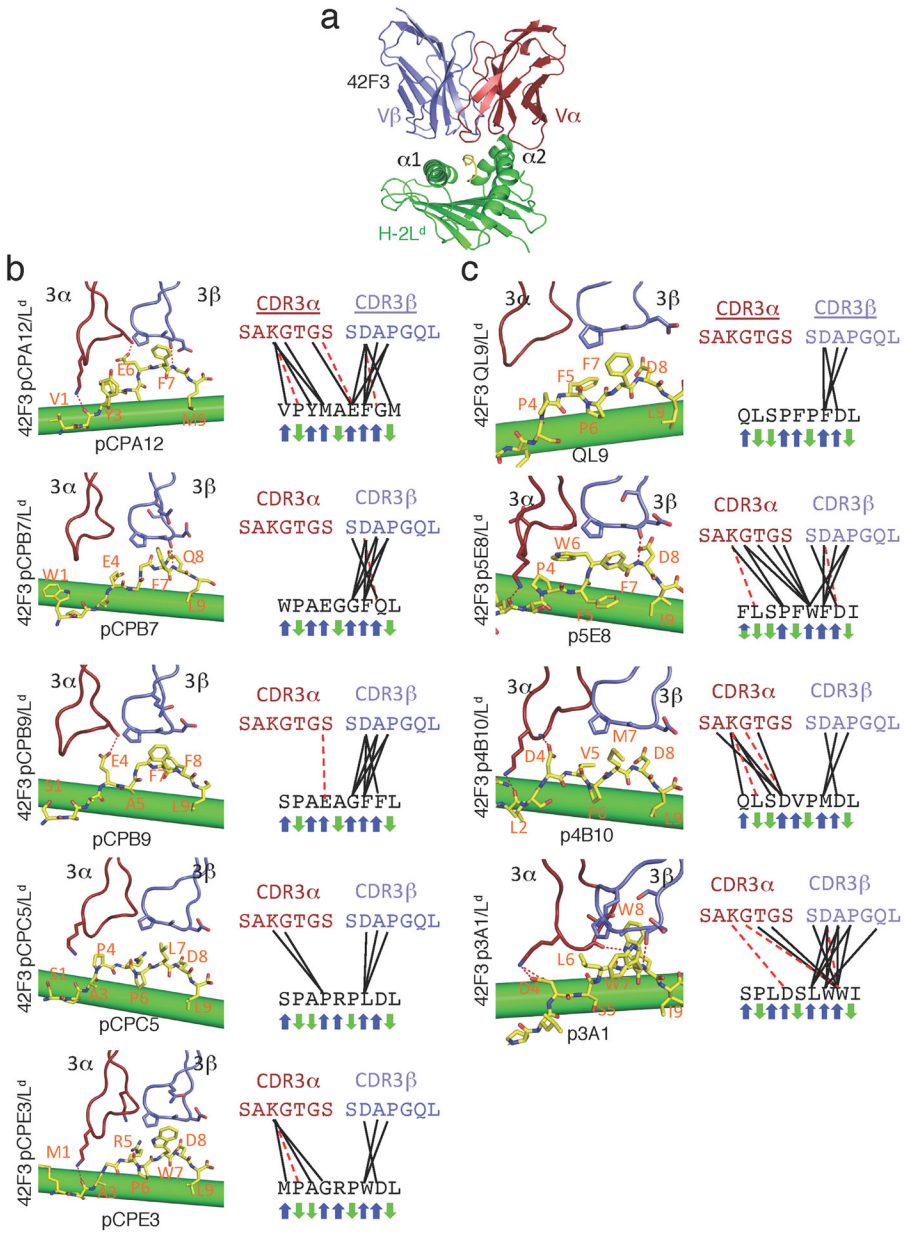

Fig. 3.

Peptide specificity of the 42F3 TCR

(**a**) The overall structure of the 42F3-QL9/H-2L^{d} complex. The MHC is illustrated in green, the TCRα in red, the TCRβ in blue and the peptide in yellow. (**b-c**) The peptide recognition by CDR3α and CDR3β loops of the 42F3 TCR for five synthetic peptides derived from the (**b**) second-generation yeast displayed library and (**c**) four from the first-generation library. Contacts are depicted as (left) structures and (right) contact maps. TCR residues making contacts to the peptides are represented as sticks. TCR CDR3 loops and the peptide identity are labeled in each panel. Black lines represent van der Waals contacts and red dashed lines represent hydrogen bonds. Blue (TCR-exposed) and green (MHC-buried) arrows illustrate the direction of the amino acid side chains on the TCR-pMHC complex.

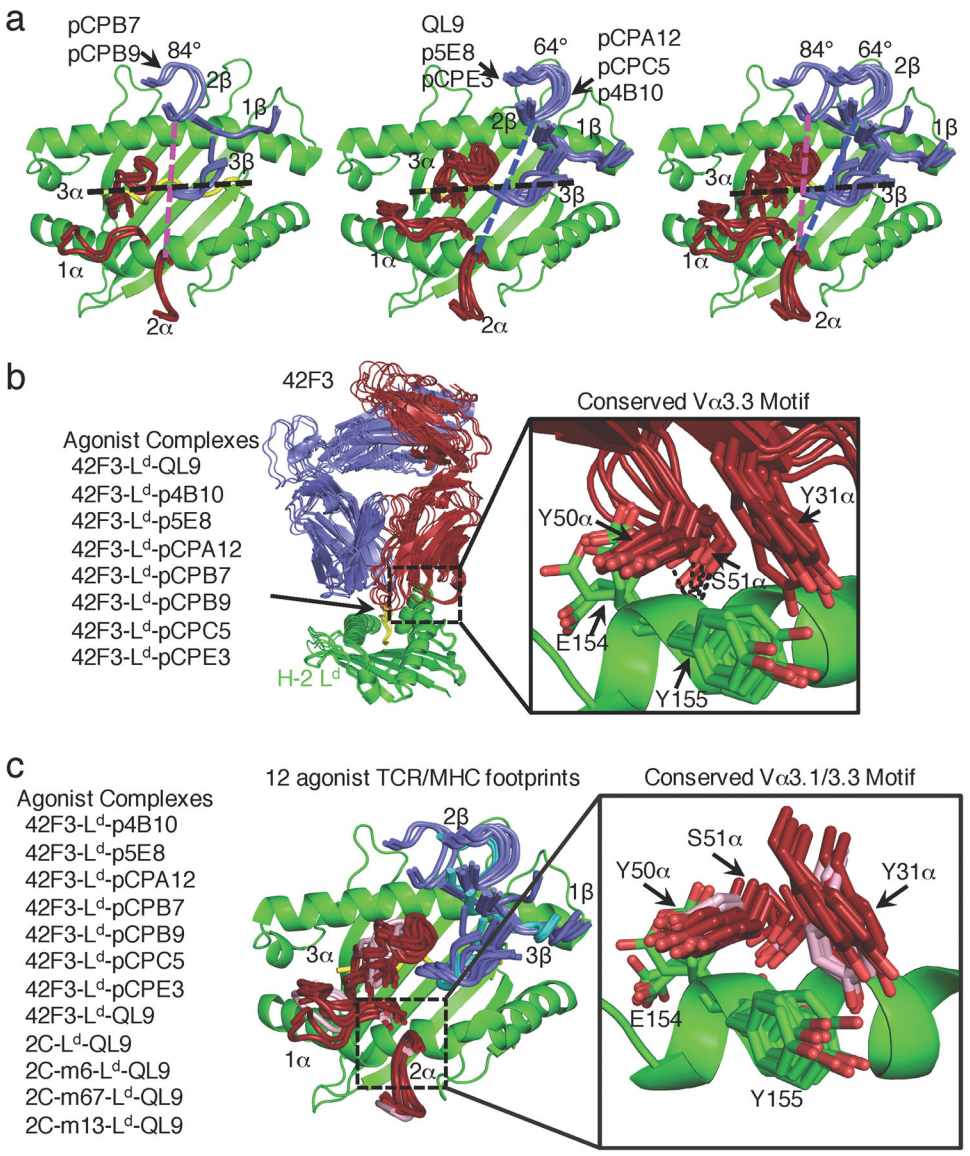

Fig. 4.

Two agonist geometries accommodated by Vα3 germline motif

(**a**) Overlaid geometric docking modes of the 42F3 TCR to H-2L^d binding at an 84° docking angle (left), 64° docking angle (center) and an overlay for comparison (right). The MHC is illustrated as a green ribbon, where the Vα CDR loops are in red and Vβ CDR loops are in blue. A black line is used to identify the QL9 peptide position and dashed colored lines are used to connect equivalent positions in CDR2α and CDR2β positions in the 84°(pink) and 64°(blue) geometries. Peptide names label the corresponding TCR-pMHC geometries. (**b**) The conserved germline contacts of the 42F3 Vα3.3 (red) to the H-2L^d α2 helix (green) across eight agonist complexes. The conserved germline contacts are inset and illustrated as sticks and dashed lines represent hydrogen bonds. (**c**) The conserved germline contacts of TCR Vα3 to the H-2L^d α2 helix (green) across twelve agonist complexes of 42F3 (red), 2C

and 2C-variants (pink). The conserved germline contacts are illustrated as sticks and dashed lines represent hydrogen bonds.

Table 1

Synthetic 42F3 Peptide Signaling and Binding Properties.

Peptide	Sequence	EC_{50} (μM)	E_{max} (IL-2 pg/ml)	*KD* (μM)*	*koff* (s^{-1})	*kon* ($M^{-1}s^{-1}$)
QL9	QLSPFPFDL	0.0447	399	40	>5.00E-01	N.D.
p4B10	QLSDVPMDL	0.000164	3297	10	>5.00E-01	N.D.
p5E8	FLSPFWFDI	1.38	3349	48	>5.00E-01	N.D.
pCPA12	VPYMAEFGM	5.95	1149	2	5.79E-02	3.14E+04
pCPC5	SPAPRPLDL	0.416	363	1	1.97E-01	2.70E+04
pCPE3	MPAGRPWDL	>100	N.D.	0.7	1.66E-01	5.86E+04
pCPB7	WPAEGGFQL	0.00286	2844	0.1	5.79E-02	4.95E+05
pCPB9	SPAEAGFFL	0.07	3144	0.1	6.68E-02	2.40E+05
p3A1	SPLDSLWWI	inactive	inactive	4	7.52E-01	2.01E+05

*Values obtained from steady-state experiment.

N.D. - Not determined